Controllability and Observability Analysis of DC Motor System and a Design of FLC-Based Speed Control Algorithm

Iswanto Suwarno [1,2,*], Yaya Finayani [3], Robbi Rahim [4], Jassim Alhamid [5], Ahmed Ramadhan Al-Obaidi [6]
[1] Department of Engineer Professional Program, Universitas Muhammadiyah Yogyakarta, Yogyakarta, Indonesia
[2] Department of Electrical Engineering, Universitas Muhammadiyah Yogyakarta, Yogyakarta, Indonesia
[3] Department of Electronics Engineering, Politeknik Pratama Mulia Surakarta, Surakarta, Indonesia
[4] Sekolah Tinggi Ilmu Manajemen Sukma, Medan, Indonesia
[5] School of Mechanical and Materials Engineering, Washington State University Tri-Cities, 2710 Crimson Way, Richland, Washington
[6] Department of Mechanical Engineering, Faculty of Engineering, Mustansiriyah University, Baghdad, Iraq
Email: [1] iswanto_te@umy.ac.id*, [3] yayafinaakbar@gmail.com, [4] usurobbi85@zoho.com, [5] Jassim.alhamid@wsu.edu, [6] ahmedram@uomustansiriyah.edu.iq
*Corresponding Author

***Abstract*— DC motor is an electrical motor widely used for industrial applications, mostly to support production processes. It is known for its flexibility and operational-friendly characteristics. However, the speed of the DC motor needs to be controlled to have desired speed performance or transient response, especially when it is loaded. This paper aims to design a DC motor model and its speed controller. First, the state space representation of a DC motor was modeled. Then, the controllability and observability were analyzed. The transfer function was made based on the model after the model was ensured to be fully controllable and observable. Therefore, a fuzzy logic controller is employed as its speed controller. Fuzzy logic controller provides the best system performance among other algorithms; the overshoot was successfully eliminated, rise time was improved, and the steady-state error was minimized. The proposed control algorithm showed that the speed controller of the DC motor, which was designed based on the fuzzy logic controller, could quickly control the speed of the DC motor. The detail of resulted system performance was 2.427 seconds of rising time, 11 seconds of settling time, and only required 12 seconds to reach the steady state. These results were proved faster and better than the system performance of PI and PID controllers.**

***Keywords*— controllability; observability; DC motor; Fuzzy logic controller; speed controller**

I. INTRODUCTION

Fuzzy logic was first published in Berkeley by Lotfi Zadeh, a professor at the University of California, in 1965. The fundamental theory of fuzzy logic is the theory of fuzzy sets. According to the theory, the role of a membership degree in defining the existence of elements in a set is profoundly important [1]. Membership values or membership degree with a membership function is the main characteristic of reasoning with fuzzy logic [2]. In many cases, fuzzy logic is utilized to map problems from input to the desired output. There are several widely-known fuzzy methods: Mamdani [3], Sugeno [4], and Tsukamoto [5].

Fuzzy logic controller is an algorithm of artificial intelligence, commonly applied to control hardware systems. FLC is the most common predictive controller [6]. In robotics, FLC has been used for induction motors [7], two-wheeled inverted pendulums [8], and UAVs [9]. In fact, many electrical and mechanical industrial components have been controlled with FLC-based controllers: electromagnetic stirrer [10], drive in drive inverter-fed [11], self-reluctance generator [12], and PMSM drive [13]. Several researchers also applied FLC for robot manipulators [14] and electrical vehicles [15][16], and even built FLC-based self-tuning actuators [17]. Moreover, FLC was also applied to overcome problems in advanced actuators, such as movement disorders in artificial neuromodulators [18]. FLC was also widely applied for longitudinal control [19] to attitude control [20]. In tracking control systems, FLC was applied for practical fixed-time tracking [21], path tracking [22], and position tracking [23]. Similarly, FLC was also widely used in navigation and coordination control systems, i.e., navigation for marine robots [24], cellular robots [25], and multi robots [26].

The development of FLC cannot be separated from other technological advances. For example, FLC has been used in many conventional power generation and distribution systems: disturbance rejection in power distribution system [27], and frequency control in power system [28]. Since then, research on FLC-based systems has rapidly increased along with the development of microgrid and renewable energy-based power generators, such as photovoltaic-based control systems [29][30] and wind turbines [31]. The most popular technique to maximize energy extraction in solar power systems is MPPT; many MPPT techniques are based on fuzzy algorithm [32][33][34]. The application is not limited to power-related systems; FLC was also proposed for the communication control of a smartgrid system [35]. Many other subsystems in microgrid systems are based on FLC: i.e., battery storage [36], reliability assessment [37], improved reliability control [38], and distributed energy management [39]. Many energy managements of varying advanced technologies used FLC: i.e., beam-pumping motor systems

[40], and heavy-duty emergency rescue vehicles [41]. Sometimes researchers even applied FLC for many purposes, as in research by Mu [42], which applied FLC for microgrid's intelligent frequency control while improving the battery storage and management system.

The rapid development and broad application of FLC are due to its nature which is similar to the logic of human beings, enabling several factors to be considered simultaneously in the decision-making process. Other intelligent algorithms, such as Neural-Network [43], can consider several factors in their decision-making process. However, it is easier to design fuzzy-based systems with a rational rule base than complex equations or weighing processes in other intelligent algorithms.

Another competitive solution is adaptive controllers, especially PI-based adaptive controllers [44]. Similarly, PID-based controllers are widely used in industrial applications. Moreover, PID-based controllers are popular for speed control of many electrical motors [45][46].

This paper specifically proposed a design of a speed control algorithm based on fuzzy logic controller algorithm for universal DC motors. DC motors were chosen due to their broad industrial applications. The modeling of DC motor considered the controllability and observability of the obtained system model. Then, the proposed speed controller of the DC motor was applied with an optimization using the membership function of error and its derivative to obtain the best rising and settling time with no overshoot in the system response. The performance results were then compared to other closed-loop control algorithms such as PID-based controllers.

II. DC MOTOR MODELING

A Servo DC motor is an electric motor supplied by a DC voltage source. There are two types of servo DC motors: brushed DC motors and brushless DC motors. Servo DC motor is one of the electric motors commonly used as industrial actuators.

The DC motor is modeled as in Fig. 1. Based on the figure, the working principle of a DC motor can be explained. A force will result when an electrical current flows in a magnetic field. The magnetic field in the DC motor can be obtained from an electromagnetic field or a permanent magnet.

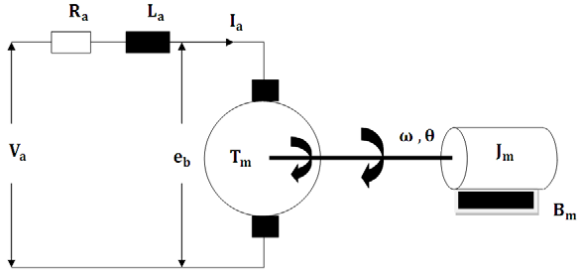

Fig. 1. A circuit of DC motor with permanent magnet

Based on Fig. 1, two modeling of DC motor can be achieved: electrical modeling and mechanical modeling. Electrical modeling can be obtained using the Kirchoff Law of Voltage, which can be written as follows,

$$V_a(t) = V_{R_a} + V_{L_a} + e_b$$

$$V_a(t) = R_a i_a(t) + L_a \frac{di_a}{dt} + e_b \quad (1)$$

where V_a is an input voltage to the DC motor, R_a is the electrical resistance, L_a is the electrical inductance, and e_b is the back electromotive force (EMF).

Meanwhile, the mathematical equation for the back electromotive force (EMF) can be expressed as follows,

$$e_b = K_b \omega(t) \quad (2)$$

where K_b is a constant for the electromotive force and $\omega(t)$ is an angular acceleration of the DC motor. The equation for the angular acceleration of the DC motor can be written as,

$$\omega(t) = \frac{d\theta}{dt} \quad (3)$$

Then, the equations for the angular acceleration and the back electromotive force of the DC motor are substituted into Equation 1 so that the following new equation can be obtained.

$$V_a(t) = R_a i_a(t) + L_a \frac{di}{dt} + K_b \frac{d\theta}{dt}$$

$$\frac{di}{dt} = \frac{V_a(t)}{L_a} - \frac{K_b \frac{d\theta}{dt}}{L_a} - \frac{R_a i_a(t)}{L_a} \quad (4)$$

On the contrary, the mechanical modeling of the DC motor can be obtained using Newton's Law. According to Fig. 1, the mechanical modeling of the DC motor can be expressed as follows,

$$\sum T = K_m i_a$$

$$J_m \frac{d^2\theta}{dt^2} + b_m \frac{d\theta}{dt} = K_m i_a$$

$$\frac{d^2\theta}{dt^2} = \frac{K_m i_a}{J_m} - \frac{b_m \frac{d\theta}{dt}}{J_m} \quad (5)$$

where J_m is the moment inertia of the rotor, $\frac{d^2\theta}{dt^2}$ is the angular acceleration of the DC motor, b_m is the coefficient of viscous friction, and K_m is the constant for motor's torque.

Linear variable equations of the DC motor, which were obtained from Equations (4) and (5), are then used to form the state variables of the DC motor. The state variables of the DC motor are defined in Equations (6), (7), and (8).

$$x_1 = \theta \tag{6}$$

$$x_2 = \frac{d\theta}{dt} \tag{7}$$

$$x_3 = i \tag{8}$$

A common equation used for state-space representation is expressed as in the equation below,

$$\dot{x} = Ax + Bu$$

$$y = Cx + Du \tag{9}$$

State-space equations consist of four components: matrix of state vectors represented as $\dot{x}$, matrix of state variables called as A, matrix of inputs which later known as$B$, and matrix of outputs known as C.

Matrices A and B in state space equations were obtained from the model of DC motor as follows,

$$\dot{x}_1 = \frac{d\theta}{dt} \tag{10}$$

$$\dot{x}_2 = \frac{d^2\theta}{dt^2} \tag{11}$$

$$\dot{x}_3 = \frac{di}{dt} \tag{12}$$

Electrical modeling in Equation (4), mechanical modeling in Equation (5), and state variables of DC motor in Equations (6)-(8) were substituted into state-space equations as in Equations (10)-(12), so that the following new equations can be obtained:

$$\dot{x}_1 = x_2 \tag{10}$$

$$\dot{x}_2 = \frac{K_m i_a}{J_m} - \frac{b_m \frac{d\theta}{dt}}{J_m} \tag{11}$$

$$\dot{x}_3 = \frac{V_a(t)}{L_a} - \frac{K_b \frac{d\theta}{dt}}{L_a} - \frac{R_a i_a(t)}{L_a} \tag{12}$$

$$\dot{x} = Ax + Bu$$

$$\begin{bmatrix} \dot{x}_2 \\ \dot{x}_3 \end{bmatrix} = \begin{bmatrix} -\frac{b_m}{J} & \frac{K_m}{J} \\ -\frac{K_b}{L_a} & -\frac{R_a}{L_a} \end{bmatrix} \begin{bmatrix} x_2 \\ x_3 \end{bmatrix} + \begin{bmatrix} 0 \\ \frac{1}{L_a} \end{bmatrix} V_a(t)$$

Based on Equations (13) – (15), the A matrix can be defined as follows

$$A = \begin{bmatrix} -\frac{b_m}{J} & \frac{K_m}{J} \\ -\frac{K_b}{L_a} & -\frac{R_a}{L_a} \end{bmatrix} \tag{16}$$

whereas B matrix is defined as

$$B = \begin{bmatrix} 0 \\ \frac{1}{L_a} \end{bmatrix} \tag{17}$$

Furthermore, the output of the system is determined as the angular speed $\omega(t)$ so that the C matrix can be defined. Therefore, the matrix of outputs can be expressed as:

$$y = Cx + Du$$

$$y = [1 \quad 0] \begin{bmatrix} x_1 \\ x_2 \\ x_3 \end{bmatrix}$$

$$C = [1 \quad 0] \tag{18}$$

The block diagram of state space representation of DC motor can be seen in Fig. 2.

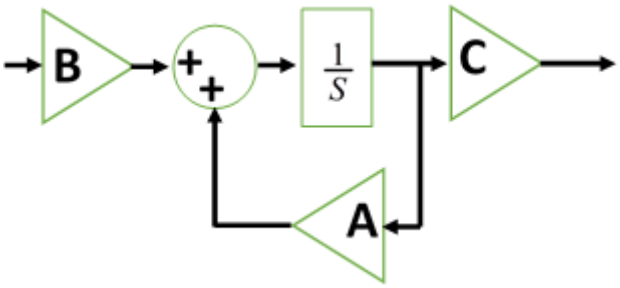

Fig. 2. A circuit of DC motor with permanent magnet

III. CONTROLLABILITY AND OBSERVABILITY

Controllability and observability hold essential roles in designing control systems with a state space. In addition, those two criteria define a complete solution for problems in control system design. Controllability and observability are two main concepts applied to modern control systems as preliminary behavior analyses of the controlled system.

Some researchers have conducted previous research on controllability and observability. For instance, Curtis et al. researched on controllability and observability of an intelligent infrastructure system [23]. The infrastructure system was modeled into a non-linear system, then analyzed for its controllability and observability using an artificial intelligence algorithm.

A. Controllability

A system is said to be controllable at t_0 if a control vector that is not limited by the system is changeable from the initial condition $x(t_0)$ to another condition for a finite time interval. Meanwhile, a system is said to be observable at t_0 if the initial condition of $x(t_0)$ is known based on the output sequence over a specified time interval.

A state-space representation of a continuous-time system is expressed as in Equation (19).

$$\dot{x}(t) = Ax(t) + Bu \tag{19}$$

Then, the controllable solution for the above equation is shown in the equation below,

$$x(t) = e^{At}x(0) + \int_0^t e^{A(t-\tau)}Bu(\tau)d\tau \tag{20}$$

For the time interval of $t_0 \leq t \leq t_1$ and the final condition as the initial points of the state space, new equations can be obtained as follows,

$$x(t_1) = e^{At_1}x(0) + \int_0^t e^{A(t-\tau)}Bu(\tau)d\tau \tag{21}$$

$$x(0) = -\int_0^t e^{A(\tau)}Bu(\tau)d\tau \tag{22}$$

By applying Silvester interpolation, the following equation can be obtained.

$$e^{At_1} = \sum_{k=0}^{n-1} \alpha_k(\tau)\, A^k \tag{23}$$

Equation (23) is then substituted into Equation (22), in which the resulted equation is written as follows,

$$x(0) = -\sum_{k=0}^{n-1} A^k B \int_0^t \alpha_k(\tau)u(\tau)d\tau \tag{24}$$

By defining the following equation,

$$\int_0^t \alpha_k(\tau)u(\tau)d\tau = \beta_k \tag{25}$$

the following equations can be obtained

$$x(0) = -\sum_{k=0}^{n-1} A^k B\, \beta_k \tag{26}$$

$$x(0) = -[A^0B \quad A^1B \quad \cdots \quad A^{n-1}B]\begin{bmatrix}\beta_k \\ \beta_k \\ \vdots \\ \beta_{n-1}\end{bmatrix} \tag{27}$$

for a $n \times n$ matrix, the controllability matrix can be.

$$[B \vdots AB \vdots \cdots \vdots A^{n-1}B] \tag{28}$$

B. Observability

Observability is profoundly important to solve unmeasurable state variables, such as a state feedback problem.

By considering an autonomous system without any control action as its input, a state-space equation for the system can be written as in the following equations.

$$\dot{x}(t) = Ax \tag{29}$$

$$y(t) = Cx \tag{30}$$

where the matrices A and C have a size of $n \times n$ and $m \times n$, respectively. The system is said to be observable if each condition of (t_0) can be known by observing the system's output $y(t)$ in a time interval of $t_0 \leq t \leq t_1$. The control action signal $u(t)$ is negated; if the control signal is included, the solution becomes as the following expressions

$$x(t) = e^{At}x(0) + \int_0^t e^{A(t-\tau)}Bu(\tau)d\tau \tag{31}$$

$$y(t) = Ce^{At}x(0) + C\int_0^t e^{A(t-\tau)}Bu(\tau)d\tau + Du \tag{32}$$

Meanwhile, the matrix of *A, B, C, D* and the control signal *u*(*t*) are known, simplifying the equations into

$$y(t) = Ce^{At}x(0) \tag{33}$$

By referring to the previous equation

$$e^{At_1} = \sum_{k=0}^{n-1} \alpha_k(t)\, A^k \tag{34}$$

the following equations can be obtained:

$$y(t) = C\sum_{k=0}^{n-1} \alpha_k(t)A^k x(0) \tag{35}$$

$$y(t) = \alpha_0(t)CA^0x(0) + \alpha_1(t)CA^1x(0) + \cdots + \alpha_{n-1}(t)CA^{n-1}x(0) \tag{36}$$

$$y(t) = [\alpha_0(t) \quad \alpha_1(t) \quad \cdots \quad \alpha_{n-1}(t)]\begin{bmatrix}CA^0 \\ CA^1 \\ \vdots \\ CA^{n-1}\end{bmatrix} \tag{37}$$

Therefore, the observability matrix can be seen as follows

$$\begin{bmatrix}C \\ CA \\ \vdots \\ CA^{n-1}\end{bmatrix} \tag{38}$$

IV. PROPOSED CONTROL STRATEGY

The state-space model needs to be transformed into a transfer function model to design the FLC-based control system as proposed in the paper.

The transfer function of a single-input-single-output system can be formulated as.

$$G(s) = \frac{Y(s)}{U(s)} \tag{39}$$

Based on the state space equation in Equation (9), the Laplace transform of the previous equation can be written as

$$sX(s) - x(0) = AX(s) + BU(s)$$

$$Y(s) = CX(s) + DU(s) \tag{40}$$

By adding the value of $x(0) = 0$, the equations can be rewritten as

$$sX(s) - AX(s) = BU(s) \tag{41}$$

$$(sI - A)X(s) = BU(s) \tag{42}$$

$$X(s) = (sI - A)^{-1}BU(s) \tag{43}$$

Equation (43) is then substituted into (40) and can be rewritten as:

$$Y(s) = [G(s)]U(s) \tag{44}$$

where

$$G(s) = C(sI - A)^{-1}B + D \tag{45}$$

Based on Equation (45), a block diagram of a fuzzy-based control algorithm can be designed and presented in Fig. 3. According to the figure, it can be seen that the FLC used two variables for its input: the error and the derivative of error. Meanwhile, the output of FLC only consists of one variable: the control signal.

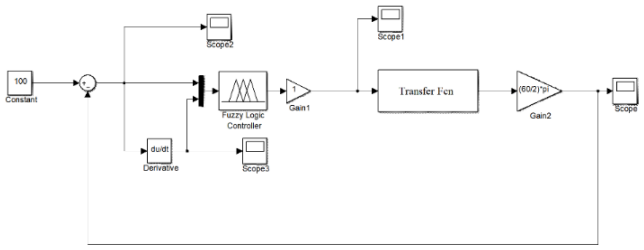

Fig. 3. A block diagram of FLC for speed control in DC motor

The proposed fully control algorithm used the fuzzy logic control algorithm with a 3×3 rule base. The rule base was designed using a lookup table of 9 rules for making decisions. The lookup table/rule base of the fuzzy logic controller is shown in Fig. 4. All rules in the rule base used the AND operator.

		Error		
		N	Z	P
D_Error	N	N	N	Z
	Z	N	Z	P
	P	Z	P	P

Fig. 4. A block diagram of FLC for speed control in DC motor

Each input and output variable of the FLC has three membership functions: Negative, Zero, and Positive, which are triangular membership functions (*trimf*). Each input and variable was also set to the range of [-10.0 10.0] and are shown in Fig. 5.

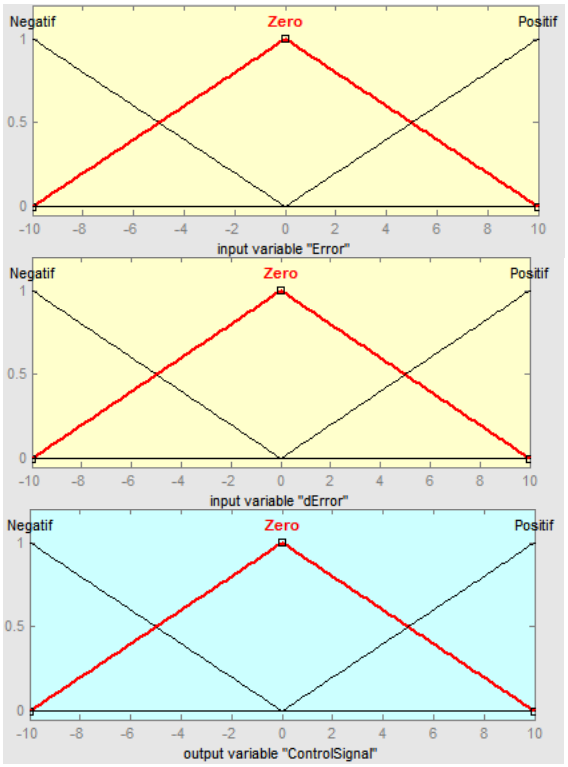

Fig. 5. Membership functions of FLC's input and output variables

Based on Fig. 5, the Negative membership function has the same domain range for all input and output variables, which is [-20 -10 0]. Similar conditions are also found in the Zero and Positive membership functions; the domain of the membership functions is the same for all input and output variables. The domain for the Zero membership function is [-10 0 10], while the domain for the Positive membership function is [0 10 20].

In the paper, the performance of speed control for DC motor using fuzzy-based algorithms is compared to the performance of PID-based controllers. The speed control system for DC motor used a PID control structure as in Fig. 6. According to the figure, it can be seen that the control system was designed based on the transfer function model, which consist of setpoint, PID control, transfer function, and position-to-RPM converter.

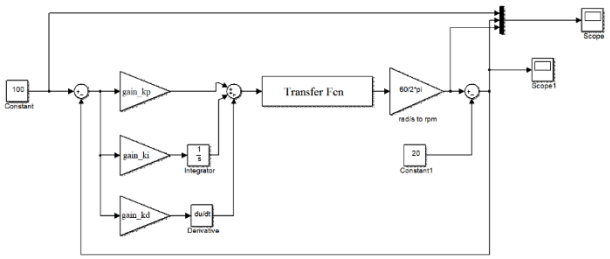

Fig. 6. A block diagram of PID controller for speed control system of DC motor

The rad-to-RPM converter shown in the figure converts the position into angular speed using a calculation expressed in Equation (46).

$$rpm = \frac{60}{2} * pi * rad \quad (46)$$

V. RESULTS AND DISCUSSIONS

The paper represented the fuzzy logic control algorithm used to control the speed of the DC motor, with a specification of DC motor listed in Table 1 [46]. The specification was used in the simulation model.

TABLE I. PARAMETERS OF DC MOTOR

Number	Parameter	Value
1	Resistance of armature, R	1 Ω
2	Inductance of armature, L	0.5H
3	Inertia of Rotor, J	0.01 kgm
4	Co-efficient of Viscous friction, b	0.1 Nms/rad
5	Torque constant, Kt	0.01Nm/A
6	Counter emf constant, Kb	0.01 s/rad

Parameters in Table 1 were then included in the state space equations in Equation 9 so that the A matrix can be obtained as follows

$$A = \begin{bmatrix} -\frac{b_m}{J} & \frac{K_m}{J} \\ -\frac{K_b}{L_a} & -\frac{R_a}{L_a} \end{bmatrix},$$

$$A = \begin{bmatrix} -10.0000 & 1.0000 \\ -0.0200 & -2.0000 \end{bmatrix}.$$

Using the same method, the B matrix can be defined as

$$B = \begin{bmatrix} 0 \\ \frac{1}{L_a} \end{bmatrix},$$

$$B = \begin{bmatrix} 0 \\ 2 \end{bmatrix}.$$

By determining the output of the DC motor as the angular speed $\omega(t)$, the C matrix can be defined as:

$$C = [1 \quad 0].$$

Thus, the components of state space equations that include the actual parameters of the DC motor are fully determined. Prior to simulation, the state-space model of the DC motor that includes the actual parameters can be analyzed further.

A system is said to be fully controllable if its composite matrix of controllability fulfills the controllability criteria, which is having a full rank. To check the controllability of a system model, the rank of the composite matrix of controllability Q_c is checked.

Referring to Equations (14) and (15), the A matrix is a 2×2 matrix while the B matrix is a 2×1. In other words, the n of the system model is 2.

Since $n = 2$, then the composite matrix of controllability (Q_c) can be defined as follows

$$(Q_c) = [B \quad AB],$$

Considering Equations (14) and (15), the following expressions can be defined.

$$B = \begin{bmatrix} 0 \\ 2 \end{bmatrix},$$

$$AB = \begin{bmatrix} -10.0000 & 1.0000 \\ -0.0200 & -2.0000 \end{bmatrix} \begin{bmatrix} 0 \\ 2 \end{bmatrix} = \begin{bmatrix} 2 \\ -4 \end{bmatrix}.$$

Therefore, the composite matrix of controllability (Q_c) of the obtained state-space model can be written as

$$(Q_c) = \begin{bmatrix} 0 & 2 \\ 2 & -4 \end{bmatrix}.$$

The rank of Q_c can be determined as follows,

$$|Q_c| = \begin{bmatrix} 0 & 2 \\ 2 & -4 \end{bmatrix} = 2$$

The rank of Q_c is 2, equal to n, and can be considered a full rank. Therefore, the system model is said to be a fully-state controllable system.

Similarly, when analyzing the controllability, the observability of a system model can be analyzed by checking the rank of the composite matrix of observability (Q_0).

Referring to Equations (14) and (16), the A matrix is a 2×2 matrix while the C matrix is a 1×2. In other words, the n of the system model is 2.

Thus, the composite matrix of observability (Q_0) can be defined as follows

$$Q_0 = [C \quad CA]^T$$

Considering Equations (14) and (16), the following expressions can be defined.

$$C = [1 \quad 0]$$

$$CA = [1 \quad 0]\begin{bmatrix} -10.0000 & 1.0000 \\ -0.0200 & -2.0000 \end{bmatrix}$$

$$CA = [-10 \quad 1]$$

Therefore, the composite matrix of observability (Q_0) of the obtained state-space model can be written as

$$|Q_0| = \begin{vmatrix} 1 & 0 \\ -10 & 1 \end{vmatrix} = 1$$

The rank of (Q_c) can be determined as follows

$$Q_0 = [C \quad CA]^T$$

The rank of Q_0 is 1, which is less than n, so that the matrix does not have a full rank. Thus, the system is not fully state observable. However, since the rank is non-zero, the system is still observable.

Since the system model is said to be controllable, it can be ensured that the system can be stabilized using a control method. Moreover, the system model is said as fully state controllable; a state of the system model can be transferred to any desired state with a reference input in a finite time interval. Referring to this definition, the system is assumed to be able to be controlled with any closed-loop control system. Therefore, it is predicted that the system model can be controlled and stabilized using PID-based controllers, since PID-based controllers are included in the closed-loop control technique.

However, the system's behavior cannot be determined only based on controllability. The system's behavior is determined by the correlation of the achieved output and the states of the system, which characterizes the system's performance. The observability of a system determines the behavior of the system.

The system model is proved to be observable; however, it is not fully observable. This means that some of the initial states of the system can be known based on the achieved or known output; some states are unmeasurable.

After the controllability and observability of the system are analyzed, the state-space model is transformed into a transfer function using Equation (45). The obtained transfer function is written as in the following equation

$$G(s) = \frac{2}{s^2 + s + 20.02}$$

Thus, the system's transfer function can be employed to apply the FLC control algorithm with the 3×3 rule base. The system's performance with the application of FLC is then compared to the system's performances of PID-based controllers: PI and PID controllers.

The simulation results are presented in Fig. 7. The setpoint for angular speed of the DC motor was set to 1 rpm for all applied controllers. As predicted by the fully state controllable behavior, the system can be stabilized using PID-based and fuzzy logic-based controllers. All of the system's responses are asymptotically stable. According to the figure, the system's responses were also quite similar; all of the responses were critically damped. No finite overshoot or undershoot was found in all of the system's responses.

However, the system's transient response with FLC as a speed controller is proven better than the transient response of PI and PID controllers. The DC motor system with PI and PID controllers showed an almost identical response in Fig. 7, presented by the overlapped curve. Moreover, it can be seen that the performance of FLC as speed control of DC motor is faster among all the applied controllers; the rising time was 2.427 seconds, the settling time was 11 seconds, and the steady-state time was 12 seconds.

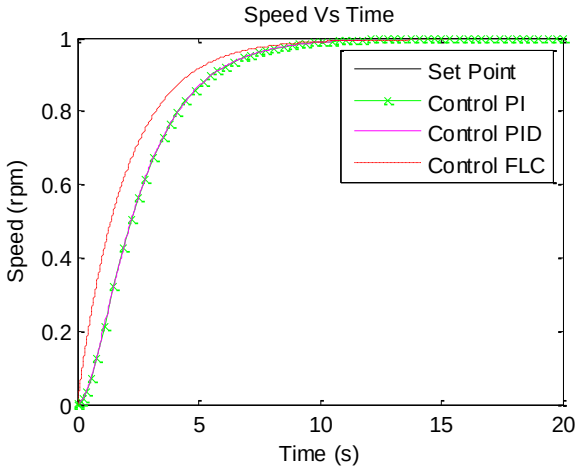

Fig. 7. Simulation results of DC motor with applied speed controllers

VI. CONCLUSIONS

The DC motor system model in the state-space model was a full state controllable system and observable system. The last development of speed control is explained in the paper using a fuzzy logic controller. In the paper, the speed control of the DC motor was tested in an undisturbed area. The paper represented the speed control of the DC motor with input as setpoints of step signal with the value of 1 rpm. The paper researched the speed control of DC motor using a fuzzy logic controller algorithm, then compared the performance results with the results of PI and PID controllers. The proposed algorithm showed that the speed of the DC motor could be controlled with a rising time of 2.427 seconds, a settling time of 12 seconds, and only 12 seconds to reach a steady state. These results were found more prominent than the results of PI and PID controllers.

REFERENCES

[1] M. A. Zaman and M. A. Razzak, "Sustainable Microgrid Analysis for Kutubdia Island of Bangladesh," IEEE Access, vol. 10, pp. 37533–37556, 2022, doi: 10.1109/ACCESS.2022.3164677.

[2] P. Nayak and B. Vathasavai, "Energy Efficient Clustering Algorithm for Multi-Hop Wireless Sensor Network Using Type-2 Fuzzy Logic," IEEE Sens. J., vol. 17, no. 14, pp. 4492–4499, Jul. 2017, doi: 10.1109/JSEN.2017.2711432.

[3] C. Saha, S. Das, K. Pal, and S. Mukherjee, "A Fuzzy Rule-Based Penalty Function Approach for Constrained Evolutionary Optimization," IEEE Trans. Cybern., vol. 46, no. 12, pp. 2953–2965, Dec. 2016, doi: 10.1109/TCYB.2014.2359985.

[4] P. Melin, O. Mendoza, and O. Castillo, "Face Recognition With an Improved Interval Type-2 Fuzzy Logic Sugeno Integral and Modular

Neural Networks," IEEE Trans. Syst. Man, Cybern. - Part A Syst. Humans, vol. 41, no. 5, pp. 1001–1012, Sep. 2011, doi: 10.1109/TSMCA.2010.2104318.

[5] L. T. H. Lan et al., "A new complex fuzzy inference system with fuzzy knowledge graph and extensions in decision making," IEEE Access, vol. 8, pp. 164899–164921, 2020, doi: 10.1109/ACCESS.2020.3021097.

[6] M. Hamdy, S. Abd-Elhaleem, and M. A. Fkirin, "Adaptive Fuzzy Predictive Controller for a Class of Networked Nonlinear Systems With Time-Varying Delay," IEEE Trans. Fuzzy Syst., vol. 26, no. 4, pp. 2135–2144, Aug. 2018, doi: 10.1109/TFUZZ.2017.2764851.

[7] M. A. Hannan, J. A. Ali, P. J. Ker, A. Mohamed, M. S. H. Lipu, and A. Hussain, "Switching Techniques and Intelligent Controllers for Induction Motor Drive: Issues and Recommendations," IEEE Access, vol. 6, no. c, pp. 47489–47510, 2018, doi: 10.1109/ACCESS.2018.2867214.

[8] J. Huang, M. Ri, D. Wu, and S. Ri, "Interval Type-2 Fuzzy Logic Modeling and Control of a Mobile Two-Wheeled Inverted Pendulum," IEEE Trans. Fuzzy Syst., vol. 26, no. 4, pp. 2030–2038, Aug. 2018, doi: 10.1109/TFUZZ.2017.2760283.

[9] A. Sarabakha, C. Fu, E. Kayacan, and T. Kumbasar, "Type-2 Fuzzy Logic Controllers Made Even Simpler: From Design to Deployment for UAVs," IEEE Trans. Ind. Electron., vol. 65, no. 6, pp. 5069–5077, Jun. 2018, doi: 10.1109/TIE.2017.2767546.

[10] S. Bicakci, M. Coramik, H. Gunes, H. Citak, and Y. Ege, "Increasing Energy Efficiency With Fuzzy Logic Control in FPGA-Based Electromagnetic Stirrer," IEEE Trans. Plasma Sci., vol. 49, no. 7, pp. 2195–2209, Jul. 2021, doi: 10.1109/TPS.2021.3090326.

[11] Z. M. Elbarbary, H. A. Hamed, and E. E. El-Kholy, "Comments on 'A Performance Investigation of a Four-Switch Three-Phase Inverter-Fed IM Drives at Low Speeds Using Fuzzy Logic and PI Controllers,'" IEEE Trans. Power Electron., vol. 33, no. 9, pp. 8187–8188, Sep. 2018, doi: 10.1109/TPEL.2017.2743681.

[12] G. P. Viajante et al., "Design and Implementation of a Fuzzy Control System Applied to a 6 × 4 SRG," IEEE Trans. Ind. Appl., vol. 57, no. 1, pp. 528–536, Jan. 2021, doi: 10.1109/TIA.2020.3037263.

[13] S. Murshid and B. Singh, "Implementation of PMSM Drive for a Solar Water Pumping System," IEEE Trans. Ind. Appl., vol. 55, no. 5, pp. 4956–4964, Sep. 2019, doi: 10.1109/TIA.2019.2924401.

[14] X. Yu, S. Zhang, Q. Fu, C. Xue, and W. Sun, "Fuzzy Logic Control of an Uncertain Manipulator With Full-State Constraints and Disturbance Observer," IEEE Access, vol. 8, pp. 24284–24295, May 2020, doi: 10.1109/ACCESS.2020.2968925.

[15] S. Wang, X. Huang, J. M. Lopez, X. Xu, and P. Dong, "Fuzzy Adaptive-Equivalent Consumption Minimization Strategy for a Parallel Hybrid Electric Vehicle," IEEE Access, vol. 7, pp. 133290–133303, 2019, doi: 10.1109/ACCESS.2019.2941399.

[16] Y. Zhang, C. Zhang, Z. Huang, L. Xu, Z. Liu, and M. Liu, "Real-Time Energy Management Strategy for Fuel Cell Range Extender Vehicles Based on Nonlinear Control," IEEE Trans. Transp. Electrif., vol. 5, no. 4, pp. 1294–1305, Dec. 2019, doi: 10.1109/TTE.2019.2958038.

[17] N. Farah et al., "A Novel Self-Tuning Fuzzy Logic Controller Based Induction Motor Drive System: An Experimental Approach," IEEE Access, vol. 7, pp. 68172–68184, 2019, doi: 10.1109/ACCESS.2019.2916087.

[18] S. Yang et al., "Design of Hidden-Property-Based Variable Universe Fuzzy Control for Movement Disorders and Its Efficient Reconfigurable Implementation," IEEE Trans. Fuzzy Syst., vol. 27, no. 2, pp. 304–318, Feb. 2019, doi: 10.1109/TFUZZ.2018.2856182.

[19] C. Chen, W.-Q. Tan, X.-J. Qu, and H.-X. Li, "A Fuzzy Human Pilot Model of Longitudinal Control for a Carrier Landing Task," IEEE Trans. Aerosp. Electron. Syst., vol. 54, no. 1, pp. 453–466, Feb. 2018, doi: 10.1109/TAES.2017.2760779.

[20] L. Sun and Z. Zheng, "Saturated Adaptive Hierarchical Fuzzy Attitude-Tracking Control of Rigid Spacecraft With Modeling and Measurement Uncertainties," IEEE Trans. Ind. Electron., vol. 66, no. 5, pp. 3742–3751, May 2019, doi: 10.1109/TIE.2018.2856204.

[21] M. Chen, H. Wang, and X. Liu, "Adaptive Fuzzy Practical Fixed-Time Tracking Control of Nonlinear Systems," IEEE Trans. Fuzzy Syst., vol. 29, no. 3, pp. 664–673, Mar. 2021, doi: 10.1109/TFUZZ.2019.2959972.

[22] C.-L. Hwang, C.-C. Yang, and J. Y. Hung, "Path Tracking of an Autonomous Ground Vehicle With Different Payloads by Hierarchical Improved Fuzzy Dynamic Sliding-Mode Control," IEEE Trans. Fuzzy Syst., vol. 26, no. 2, pp. 899–914, Apr. 2018, doi: 10.1109/TFUZZ.2017.2698370.

[23] Z. Lin, T. Zhang, Q. Xie, and Q. Wei, "Intelligent Electro-Pneumatic Position Tracking System Using Improved Mode-Switching Sliding Control With Fuzzy Nonlinear Gain," IEEE Access, vol. 6, pp. 34462–34476, 2018, doi: 10.1109/ACCESS.2018.2847637.

[24] N. A. A. Hussain, S. S. A. Ali, M. Ovinis, M. R. Arshad, and U. M. Al-Saggaf, "Underactuated Coupled Nonlinear Adaptive Control Synthesis Using U-Model for Multivariable Unmanned Marine Robotics," IEEE Access, vol. 8, pp. 1851–1865, 2020, doi: 10.1109/ACCESS.2019.2961700.

[25] M. Faisal, M. Algabri, B. M. Abdelkader, H. Dhahri, and M. M. Al Rahhal, "Human Expertise in Mobile Robot Navigation," IEEE Access, vol. 6, pp. 1694–1705, 2018, doi: 10.1109/ACCESS.2017.2780082.

[26] Y.-C. Chang et al., "Interpretable Fuzzy Logic Control for Multirobot Coordination in a Cluttered Environment," IEEE Trans. Fuzzy Syst., vol. 29, no. 12, pp. 3676–3685, Dec. 2021, doi: 10.1109/TFUZZ.2021.3111446.

[27] X. Zhou, Y. Cui, and Y. Ma, "Fuzzy Linear Active Disturbance Rejection Control of Injection Hybrid Active Power Filter for Medium and High Voltage Distribution Network," IEEE Access, vol. 9, pp. 8421–8432, 2021, doi: 10.1109/ACCESS.2021.3049832.

[28] A. O. Aluko, R. P. Carpanen, D. G. Dorrell, and E. E. Ojo, "Robust State Estimation Method for Adaptive Load Frequency Control of Interconnected Power System in a Restructured Environment," IEEE Syst. J., vol. 15, no. 4, pp. 5046–5056, Dec. 2021, doi: 10.1109/JSYST.2020.3005979.

[29] P. K. Pardhi, S. K. Sharma, and A. Chandra, "Control of Single-Phase Solar Photovoltaic Supply System," IEEE Trans. Ind. Appl., vol. 56, no. 6, pp. 7132–7144, Nov. 2020, doi: 10.1109/TIA.2020.3024171.

[30] P. K. Pardhi and S. K. Sharma, "High Gain Non Isolated DC Converter Employed in Single-Phase Grid-Tied Solar Photovoltaic Supply System," IEEE Trans. Ind. Appl., vol. 57, no. 5, pp. 5170–5182, Sep. 2021, doi: 10.1109/TIA.2021.3095439.

[31] S. Puchalapalli and B. Singh, "A Single Input Variable FLC for DFIG-Based WPGS in Standalone Mode," IEEE Trans. Sustain. Energy, vol. 11, no. 2, pp. 595–607, Apr. 2020, doi: 10.1109/TSTE.2019.2898115.

[32] K. Yung Yap, C. R. Sarimuthu, and J. Mun-Yee Lim, "Artificial Intelligence Based MPPT Techniques for Solar Power System: A review," J. Mod. Power Syst. Clean Energy, vol. 8, no. 6, pp. 1043–1059, 2020, doi: 10.35833/MPCE.2020.000159.

[33] N. Priyadarshi, S. Padmanaban, J. B. Holm-Nielsen, F. Blaabjerg, and M. S. Bhaskar, "An Experimental Estimation of Hybrid ANFIS–PSO-Based MPPT for PV Grid Integration Under Fluctuating Sun Irradiance," IEEE Syst. J., vol. 14, no. 1, pp. 1218–1229, Mar. 2020, doi: 10.1109/JSYST.2019.2949083.

[34] M. Aly and H. Rezk, "A Differential Evolution-Based Optimized Fuzzy Logic MPPT Method for Enhancing the Maximum Power Extraction of Proton Exchange Membrane Fuel Cells," IEEE Access, vol. 8, pp. 172219–172232, 2020, doi: 10.1109/ACCESS.2020.3025222.

[35] K. P. Inala, B. Sah, P. Kumar, and S. K. Bose, "Impact of V2G Communication on Grid Node Voltage at Charging Station in a Smart Grid Scenario," IEEE Syst. J., vol. 15, no. 3, pp. 3749–3758, Sep. 2021, doi: 10.1109/JSYST.2020.3007320.

[36] M. Faisal, M. A. Hannan, P. J. Ker, and M. N. Uddin, "Backtracking Search Algorithm Based Fuzzy Charging-Discharging Controller for Battery Storage System in Microgrid Applications," IEEE Access, vol. 7, pp. 159357–159368, 2019, doi: 10.1109/ACCESS.2019.2951132.

[37] I. Akhtar, S. Kirmani, and M. Jameel, "Reliability Assessment of Power System Considering the Impact of Renewable Energy Sources Integration Into Grid With Advanced Intelligent Strategies," IEEE Access, vol. 9, pp. 32485–32497, 2021, doi: 10.1109/ACCESS.2021.3060892.

[38] S. M. Said, M. Aly, B. Hartmann, A. G. Alharbi, and E. M. Ahmed, "SMES-Based Fuzzy Logic Approach for Enhancing the Reliability

of Microgrids Equipped With PV Generators," IEEE Access, vol. 7, pp. 92059–92069, 2019, doi: 10.1109/ACCESS.2019.2927902.

[39] M. Jafari, Z. Malekjamshidi, J. Zhu, and M.-H. Khooban, "A Novel Predictive Fuzzy Logic-Based Energy Management System for Grid-Connected and Off-Grid Operation of Residential Smart Microgrids," IEEE J. Emerg. Sel. Top. Power Electron., vol. 8, no. 2, pp. 1391–1404, Jun. 2020, doi: 10.1109/JESTPE.2018.2882509.

[40] Y. Wang, H. H. Eldeeb, H. Zhao, and O. A. Mohammed, "Sectional Variable Frequency and Voltage Regulation Control Strategy for Energy Saving in Beam Pumping Motor Systems," IEEE Access, vol. 7, pp. 92456–92464, 2019, doi: 10.1109/ACCESS.2019.2927525.

[41] J. Xue, Q. Tu, M. Pan, X. Lai, and C. Zhou, "An Improved Energy Management Strategy for 24t Heavy-Duty Hybrid Emergency Rescue Vehicle With Dual-Motor Torque Increasing," IEEE Access, vol. 9, pp. 5920–5932, 2021, doi: 10.1109/ACCESS.2020.3048343.

[42] C. Mu, Y. Zhang, H. Jia, and H. He, "Energy-Storage-Based Intelligent Frequency Control of Microgrid With Stochastic Model Uncertainties," IEEE Trans. Smart Grid, vol. 11, no. 2, pp. 1748–1758, Mar. 2020, doi: 10.1109/TSG.2019.2942770.

[43] S. Wang, H. Yu, J. Yu, J. Na, and X. Ren, "Neural-Network-Based Adaptive Funnel Control for Servo Mechanisms With Unknown Dead-Zone," IEEE Trans. Cybern., vol. 50, no. 4, pp. 1383–1394, Apr. 2020, doi: 10.1109/TCYB.2018.2875134.

[44] K. Y. Ahmed, N. Z. Bin Yahaya, V. S. Asirvadam, N. Saad, R. Kannan, and O. Ibrahim, "Development of Power Electronic Distribution Transformer Based on Adaptive PI Controller," IEEE Access, vol. 6, no. c, pp. 44970–44980, 2018, doi: 10.1109/ACCESS.2018.2861420.

[45] Y. Raziyev, R. Garifulin, A. Shintemirov, and T. D. Do, "Development of a Power Assist Lifting Device With a Fuzzy PID Speed Regulator," IEEE Access, vol. 7, pp. 30724–30731, 2019, doi: 10.1109/ACCESS.2019.2903234.

[46] T. Tarannum, "Intelligent Speed Control of DC Motor using ANFIS D Controller," in 2019 1st International Conference on Advances in Science, Engineering and Robotics Technology (ICASERT), May 2019, vol. 2019, no. Icasert, pp. 1–5, doi: 10.1109/ICASERT.2019.8934620.